Short communication

Electrochemical Studies on the Corrosion of Electrically Conductive Sulfide Minerals in High Pressure Hydrothermal Fluids - a Case Study From Pyrite

Sen Lin, Heping Li[*], Can Cui

Key Laboratory for High Temperature & High Pressure Study of the Earth's Interior, Institute of Geochemistry, Chinese Academy of Sciences, Guiyang, 550081, China
[*]E-mail: liheping@vip.gyig.ac.cn

Electrochemical data concerning electrically conductive sulfide minerals submitted to high pressure hydrothermal fluids above 150 °C has not been reported in spite of its significance. In this work, electrochemical impedance spectroscopy (EIS) and Tafel studies of pyrite corrosion in pure water, 3.5% NaCl solution and 0.1 M sulfuric acid with 1796 kPa O_2 at 350 °C, 30 MPa were conducted, with the assistance of a self-designed three-electrode electrochemical measurement set-up that can operate in high pressure hydrothermal fluids. Results show that in pure water, 3.5% NaCl solution, and 0.1 M sulfuric acid with 1796 kPa O_2, corrosion potential (E_{corr}) is respectively -150, -334 and -752 mV, corrosion current (I_{corr}) is respectively 1.44E-5, 1.95E-4 and 7.73E-3 A. The solid-liquid interface information at pyrite surface achieved by EIS measurements reveals an important reason of the difference between the values of E_{corr} and I_{corr} in the three studied fluids. The electrochemical studies in this work also provide a promising method for research into the corrosion of other conductive sulfide minerals in high pressure hydrothermal fluids.

1. INTRODUCTION

Sulfide minerals, most of which are electrically conductive, are important raw mineral materials for metals such as Cu, Pb, Zn, Au, and Ag. The corrosion of sulfide minerals in high pressure hydrothermal fluids is a crucial topic in the research of submarine hydrothermal deposit and high temperature hydrometallurgy. The corrosion of sulfide minerals in submarine hydrothermal fluids plays an important role in the formation of a variety of ore deposits as it not only provided metallogenic material for the ore-forming events [1-3], but also adjusted the Eh and pH value of the

ore-forming hydrothermal fluids [4]. In high temperature hydrometallurgy, pressure leaching at elevated temperatures is an effective and low-pollution way in sulfide minerals metallurgy [5], pressure leaching of pyrite [6], chalcopyrite [7,8] has been put into practice for decades.

Pyrite is the most abundant sulfide mineral on the Earth, it is also an important gold bearing mineral in metallurgy [9,10]. Corrosion of pyrite in high pressure hydrothermal fluids have been studied by previous researchers. Bailey and Peters [11] proposed that the corrosion of pyrite in hydrothermal fluids could be represented by the following two competing reactions:

$$FeS_2 + 3.5O_2 + H_2O \longrightarrow FeSO_4 + H_2SO_4$$

$$FeS_2 + 2O_2 \longrightarrow FeSO_4 + S$$
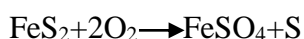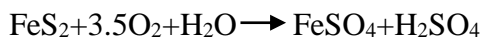
Then the products undergo further step reactions according to the hydrothermal condition, i.e., Fe(II) can be oxidized to Fe(III), Fe(III) hydrolyzes into ferric oxide or basic ferric sulfate as precipitation, and sulfur hydrolyzes into hydrogen sulfide and sulfate ions [7,13,14]. The corrosion kinetics has also been investigated [11,12,14], effects of temperature, particle size, oxygen partial pressure, and pulp density were considered. The reaction order with respect to oxygen partial pressure was found to be 0.5 at temperatures above 170°C, indicating an electrochemical mechanism [11,14].

In previous work, the researchers conducted their research mainly by examining the changes in the amount of pyrite and the solution species before and after the corrosion. Such method is intuitionistic, but not so ideal in some way. Firstly, solid-liquid interface is the place where the corrosion takes place, information of such interface is crucial in understanding the corrosion mechanism, unfortunately, the method performed by previous researchers gave little information about the solid-liquid interface. Secondly, previous investigators measured the amount of species in the hydrothermal fluids and residual pyrite after cooling down, however, uncertain variation would take place in the cooling process, which could introduce errors in the experiment results.

Electrochemical measurements technique is a powerful in-situ tool for corrosion research, electrochemical measurements such as Tafel study, electrochemical impedance spectroscope (EIS), give detailed information of corrosion process, especially the information of liquid-solid interface. Electrochemical measurements technique has already been widely employed in the study of pyrite corrosion at room temperature [15-19]. Unfortunately, there was no report of electrochemical investigation into pyrite or any other sulfide minerals, which are fragile and nonplastic, in high pressure hydrothermal fluids above 150 °C so far, though such technique has already been applied in metal corrosion research at elevated temperatures [20-23].

In this work, electrochemical studies of pyrite were conducted at 350 °C, 30 MPa with the aid of a self-designed electrochemical measurement set-up that can be applied in high pressure hydrothermal fluids. Tafel and EIS measurements were recorded respectively in pure water, 3.5% NaCl solution (simulated seawater), 0.1M sulfuric acid with 1796 kPa O_2 (fluid appearing in acid pressure leaching). The electrochemical parameters and pyrite-liquid interface were considered using achieved electrochemical data.

2. EXPERIMENTAL

The electrochemical measurements were performed in a self-designed autoclave with three electrodes (Fig. 1). The autoclave was made of titanium alloy. A resistance furnace was used to heat

the autoclave, the temperature was controlled to $\pm$ 0.5 °C by a temperature controller, and the measuring junction of the thermocouple was placed near the pyrite sample. The pressure in the system was measured by a pressure sensor, and controlled by a high pressure pump.
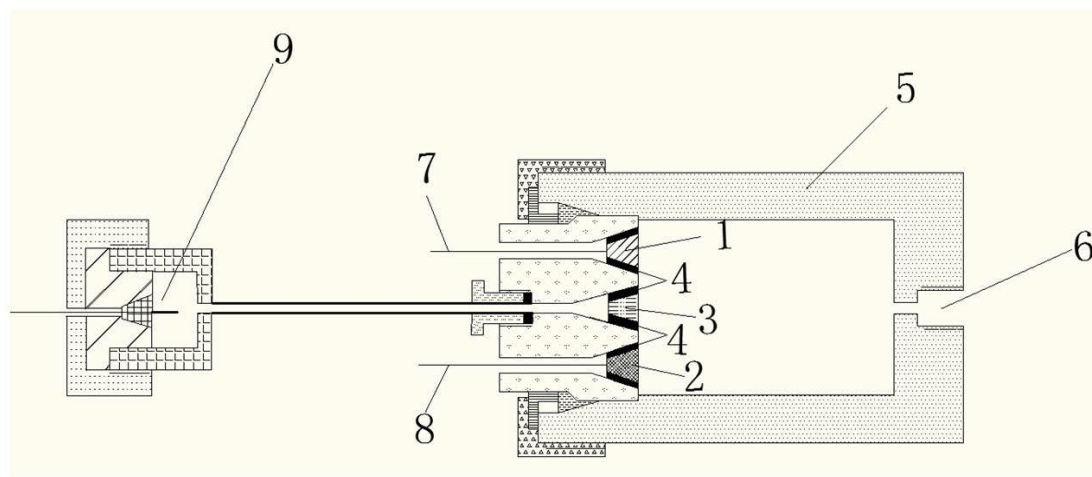
Figure 1. Schematic of the electrochemical measurement set-up with pyrite working electrode (1), ceramics-Pt counter electrode (2), porous zirconia ceramics (3), pyrophyllite taper sleeve (4), titanium alloy autoclave (5), threaded hole connecting to the pressure sensor and high pressure pump (6), silver wire connected to working electrode (7), silver wire connected to counter electrode (8), and external Ag/AgCl reference electrode (9).

The working electrode was a massive monocrystal pyrite, shaped into cone frustum with the aid of a lathe. The counter electrode was a self-made alumina ceramic cone frustum with a platinum wire in its central axis, platinum power was sintered onto its end surface to achieve sufficient counter electrode surface area. A self-designed external pressure balanced Ag/AgCl electrode filled with 0.1 M KCl was applied as the reference electrode. In present work, the calibrated equation of the electrode potential was following [24]:

$$\Delta E_{\text{SHE}} = \Delta E_{\text{obs}} + 286.6 - \Delta T + 1.745 \times 10^{-4}\Delta T^2 - 3.03 \times 10^{-6}\Delta T^3 \text{ (mV)}$$

All potential mentioned in this work was normalized with respect to the saturated hydrogen electrode (SHE) using the formula above. The working and counter electrodes were sealed up and insulated from the autoclave using pyrophyllite taper sleeve, which has high stability and high electric insulating performance after heat treatment. The pyrite working electrode was primarily polished with 2500-grit silicon carbide abrasive paper, then washed with alcohol and deionized water. High temperature silver conductive paste was employed to connect the electrodes with silver wires. All conducting wires were insulated from the autoclave by alumina ceramic tubes.

Before the autoclave was heated, high purity argon was introduced into the autoclave to drive the air out, with the purpose of avoiding the oxidation of pyrite in air when heated. When the system was heated to 350 °C, experimental solutions, deaerated by high purity argon, were pumped into the autoclave with the aid of a high pressure pump until the pressure in the autoclave reached 30 MPa.

The electrochemical measurements were conducted using a Princeton 2263A electrochemical test station and Powersuit software. EIS studies at open circuit potential was performed 1 h after the solutions were pumped in, the AC amplitude was 10 mV. Tafel studies were conducted after the EIS tests, the scan was ranged from -250 to 250 mV relative to the open circuit potential at a scan rate of 1 mV/s. Software ZSimpWin and CorrView were employed to fit the EIS and Tafel data, respectively. All chemical reagents used in this work were of analytical grade.

3. RESULTS AND DISCUSSION

EIS and Tafel studies of pyrite were conducted at 350 °C, 30 MPa. Fig. 2, 3, and 4 show the Nyquist and Bode plots of pyrite respectively in pure water, 3.5% NaCl solution, and 0.1M sulfuric acid with 1796 kPa O_2. The Bode phase plots reveal two time constants corresponding to two faradaic relaxation processes for the pyrite electrode in the three studied high pressure hydrothermal fluids. The equivalent circuit shown in Fig. 5 was employed to fit the experimental data, which includes the ohmic resistances in the electrochemical circuits (R_s) in series with two RC time constants CPE_{ct}/R_{ct} and CPE_{pf}/R_{pf}. CPE_{ct} represents the double-layer capacitance, R_{ct} is the charge transfer resistance, while, CPE_{pf}/R_{pf} represents the capacitance and resistance behaviors of the passive film. The passive film may be composed of elemental sulfur and iron oxide species, depending on solution acidity and oxidation-reduction state [12,14]. CPE is the constant phase angle element to replace the interfacial capacitance, which is defined as [25]:

$$CPE = Y_0(j\omega)^{n'} = Y_0\omega^{n'}\cos\frac{n\pi}{2} + jY_0\omega^{n'}\sin\frac{n\pi}{2}$$

Where Y_0 is a constant depending on the electrode potential, and n' is the frequency power. The interfacial capacitance C can be obtain though the following equation [26]:

$$C = Y_0(\omega_m)^{n'-1}$$

ω_m is the angular frequency at which the imaginary part of the impedance has a maximum.
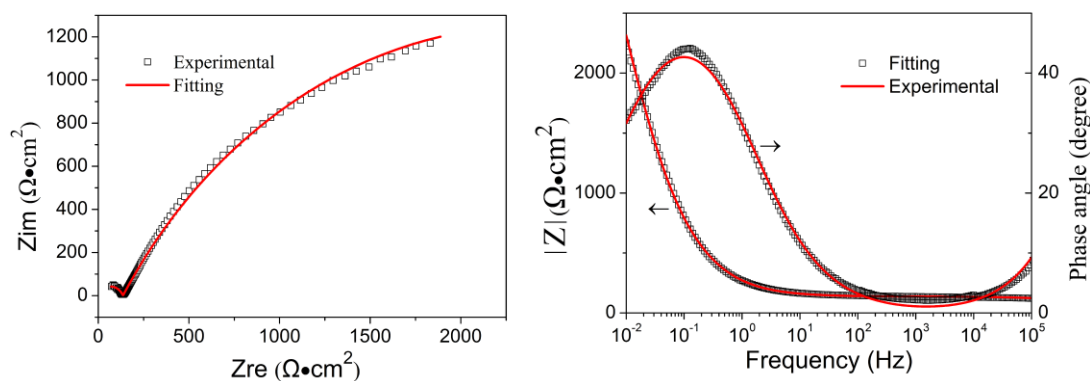
Figure 2. Nyquist and Bode plots for pyrite at open circuit potential after exposing in pure water at 350°C, 30 MPa for 1 h.
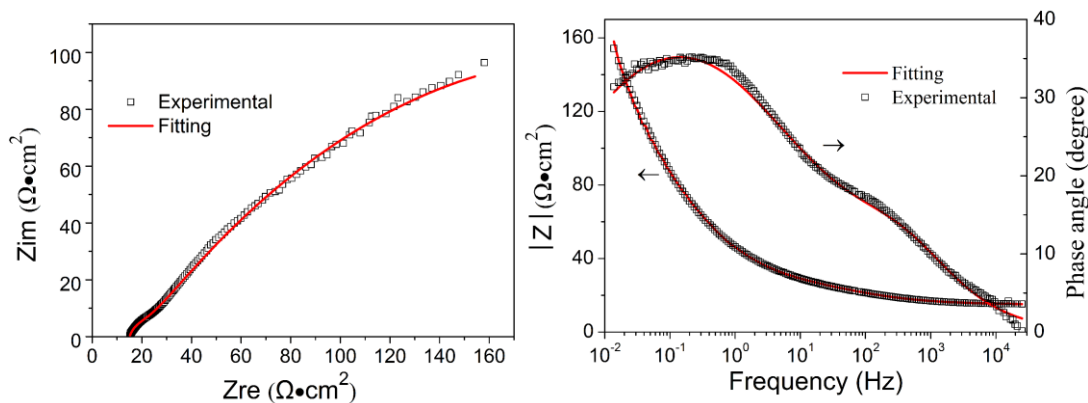
Figure 3. Nyquist and Bode plots for pyrite at open circuit potential after exposing in 3.5% NaCl solution at 350°C, 30 MPa for 1 h.
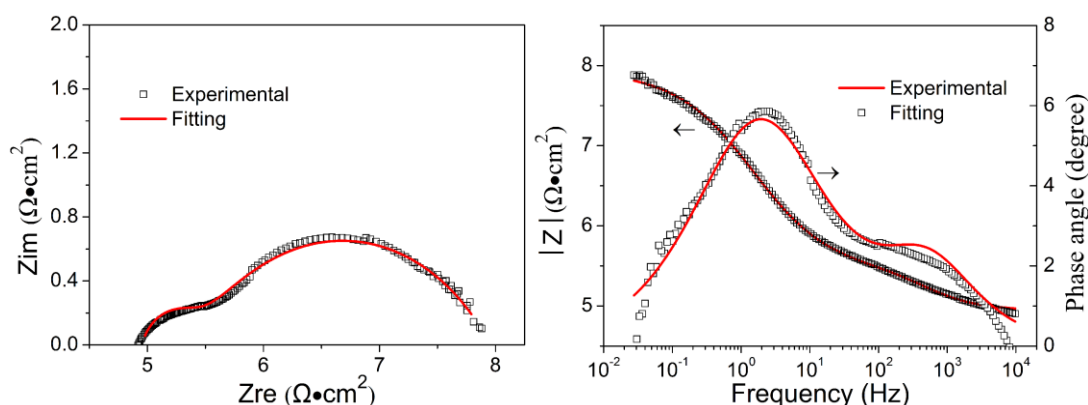
Figure 4. Nyquist and Bode plots for pyrite at open circuit potential after exposing in 0.1 M sulfuric acid with 1796 kPa O_2 at 350°C, 30 MPa for 1 h.
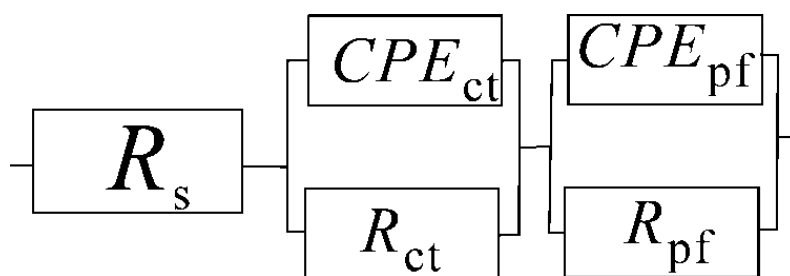
Figure 5. The equivalent circuit used in the present work for pyrite corrosion at 350 °C, 30 MPa.

The EIS fitting results were shown in Table 1. It can be seen that, in pure water, 3.5% NaCl solution, and 0.1 M sulfuric acid with 1796 kPa O_2, R_{ct} is respectively 4519, 383.2 and 2.52 $\Omega \cdot cm^2$, R_{pf} is respectively 136.3, 12.58 and 0.49 $\Omega \cdot cm^2$. In pure water, the pyrite electrode exhibited the highest value of both R_{ct} and R_{pf}, while, in 0.1 M sulfuric acid with 1796 kPa O_2, the pyrite electrode presented the lowest value of both R_{ct} and R_{pf} in the three studied fluids.

Table 1. Impedance parameters of pyrite at 350 °C, 30 MPa.

| | R_s ($\Omega \cdot cm^2$) | CPE_{ct} | | | R_{ct} ($\Omega \cdot cm^2$) | CPE_{pf} | | | R_{pf} ($\Omega \cdot cm^2$) |
		Y_0	n	C (F/cm^2)		Y_0	n	C (F/cm^2)	
Pure water	58.23	1.75E-3	0.64	3.24E-3	4519	1.38E-7	0.69	3.89E-9	136.3
3.5% NaCl	14.82	1.12E-2	0.77	1.62E-2	383.2	1.26E-3	0.42	5.83E-5	12.58
0.1 M H$_2$SO$_4$	4.94	0.11	0.60	8.34E-2	2.52	4.27E-3	0.77	9.81E-4	0.49

Fig. 6 shows the Tafel plots for pyrite in different fluids at 350 °C, 30 MPa. Information such as corrosion potential (E_{corr}), corrosion current (I_{corr}), Tafel slope (β_a, β_c) were drawn from Tafel fitting, the results were shown in Table 2. In pure water, 3.5% NaCl solution, and 0.1 M sulfuric acid, E_{corr} is respectively -150, -334 and -752 mV, I_{corr} is respectively 1.44E-5, 1.95E-4 and 7.73E-3 A.
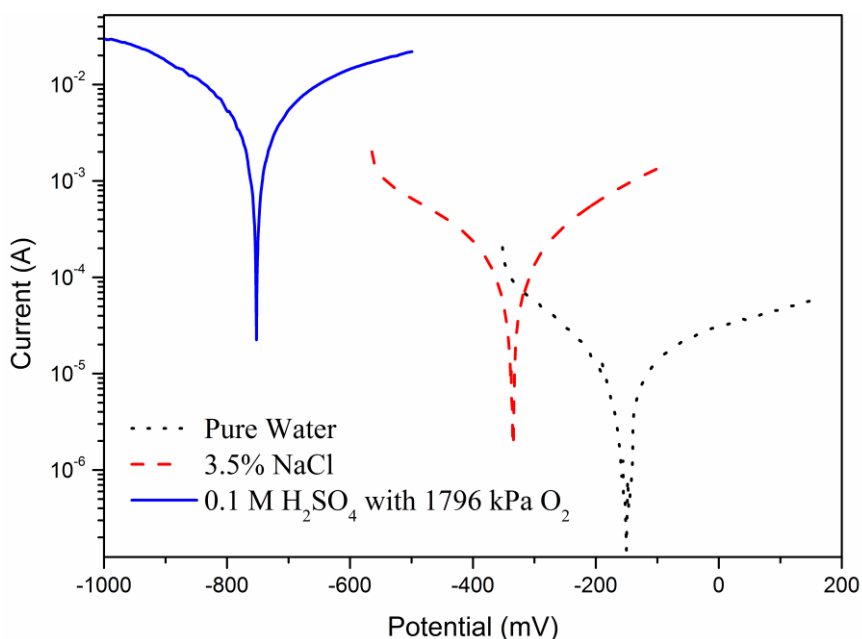
Figure 6. Tafel plots for pyrite respectively in pure water, 3.5% NaCl, and 0.1 M sulfuric acid with 1796 kPa O$_2$ at 350 °C, 30 MPa.

Table 2. Electrochemical kinetic parameters of pyrite at 350 °C, 30 MPa.

	E_{corr} (mV)	I_{corr}(A)	β_a (mV/decade)	β_c (mV/decade)
Pure water	-150	1.44E-5	87.61	502.5
3.5% NaCl	-334	1.95E-4	124.6	130.9
0.1 M H$_2$SO$_4$	-752	7.73E-3	274.8	133.1

The EIS and Tafel studies show that, compared with the conditions in pure water, the addition of 3.5% NaCl promotes the corrosion of pyrite. The effect of chloride ion has been well established by

former researchers, chloride ion is a relative strong Lewis base, it adsorbs onto the passive film, forming chloride-containing iron complexes [27], which then dissolve into the solution, result in weakening of the passive film. The opinion is confirmed by the EIS study that the fitting result of R_{pf} is 136.3 $\Omega \cdot cm^2$ in pure water, while, this value decreases to 12.58 $\Omega \cdot cm^2$ in 3.5% NaCl. In 0.1 M sulfuric acid with 1796 kPa O_2, the iron in the corrosion products tends to dissolve into the fluid, leaving elemental sulfur the only factor responsible for passivation of the pyrite electrode, thus, the value of R_{pf} is only 0.49 $\Omega \cdot cm^2$. I_{corr} represents the corrosion rate of the electrode, supposing that pyrite corrosion had a same electron transfer number in the three studied fluids, the corrosion rate in 0.1 M sulfuric acid with 1796 kPa O_2 was 39.6 times faster than in 3.5% NaCl solution, 537 times faster than in pure water.

4. CONCLUSIONS

The results of this study demonstrate the application of electrochemical measurements as a research tool for pyrite corrosion in high pressure hydrothermal fluids.

In this study, the electrochemical measurements for pyrite corrosion in pure water, 3.5% NaCl solution and 0.1 M sulfuric acid with 1796 kPa O_2 at 350 °C, 30 MPa showed that pyrite corroded the most quickly in 0.1 M sulfuric acid with 1796 kPa O_2, while, the most slowly in pure water. Electrochemical parameters such as CPE_{ct}, R_{ct}, CPE_{pf}, R_{pf}, E_{corr}, and I_{corr} for pyrite corrosion in high pressure hydrothermal fluids above 150 °C were revealed for the first time, which reflected the reaction kinetics and pyrite-liquid interface information. The electrochemical measurements for pyrite in this work also provide a promising method for studies into the corrosion of other conductive sulfide minerals in high pressure hydrothermal fluids.

References

1. P.M. Herzig, M.D. Hannington, *Ore Geol. Rev.*, 10 (1995) 95.
2. K.H. Yang, S.D. Scott, *Nature*, 383 (1996) 420.
3. R.H. James, H. Elderfield, *Geology*, 24 (1996) 1147.
4. H. Ohmoto, *Ore Geol. Rev.*, 10 (1996) 135.
5. B. Xu, Y.B. Yang, Q. Li, T. Jiang, S.Q. Liu, G.H. Li, *Miner. Eng.*, 89 (2016) 138.
6. V.G. Papangelakis, G.P. Demopoulos, *Hydrometallurgy*, 26 (1991) 309.
7. R.G. McDonald, D.M. Muir, *Hydrometallurgy*, 86 (2007) 191.
8. R.G. McDonald, D.M. Muir, *Hydrometallurgy*, 86 (2007) 206.
9. C. Gasparrini, *CIM Bull.*, 76 (1983) 144.
10. G.P. Demopoulos, V.G. Papangelakis, *CIM Bull.*, 80 (1987) 103.
11. L.K. Bailey, E. Peters, *Can. Metall. Q.*, 15 (1976) 333.

12. K. Tozawa, K. Sasaki, *Iron Control in Hydrometallurgy*, Wiley (1986) New York, US.
13. H. Ohmoto, K.I. Hayashi, Y. Kajisa, *Geochim. Cosmochim. Acta*, 58 (1994) 2169.
14. H. Long, D.G. Dixon, *Hydrometallurgy*, 73 (2004) 335.
15. P.R. Holmes, F.K. Crundwell, *Geochim. Cosmochim. Acta*, 64 (2000) 263.
16. D.P. Tao, P.E. Richardson, G.H. Luttrell, R.H. Yoon, *Electrochim. Acta*, 48 (2003) 3615.
17. L.J. Bryson, F.K. Crundwell, *Hydrometallurgy*, 143 (2014) 42.
18. B. Guo, Y.J. Peng, G. Parker, *Miner. Eng.*, 92 (2016) 78.
19. L.Y. Wang, Q.Y. Liu, K. Zheng, H.P. Li, *J. Environ. Qual.*, 45 (2016) 1344.
20. D.J. Kim, H.C. Kwon, H.P. Kim, *Corros. Sci.*, 50 (2008) 1221.
21. F. Scenini, G. Palumbo, N. Stevens, A. Cook, A. Banks, *Corros. Sci.*, 87 (2014) 71.
22. A. Krausova, J. Macak, P. Sajdl, R. Novotny, V. Renciukova, V. Vrtilkova, *J. Nucl. Mater.*, 467 (2015) 302.
23. J.Z. Wang, J.Q. Wang, E.H. Han, *J. Mar. Sci. Technol.*, 32 (2016) 333.
24. D.D. Macdonald, A.C. Scott, P. Wentrcek, *J. Electrochem. Soc.*, 126 (1979) 908.
25. F. Alcaide, E. Brillas, P.L. Cabot, *J. Electroanal. Chem.*, 547 (2003) 61.
26. C.H. Hsu, F. Mansfeld, *Corrosion*, 57 (2001) 747.
27. K. Ding, W.E. Seyfried, *Geochim. Cosmochim. Acta*, 56 (1992) 368l.